

# Chapter 20

## Pedestrian Dynamics in Jamology

Daichi Yanagisawa

**Abstract** In this paper, some achievements of research on pedestrian dynamics in Jamology are reviewed. The author focuses on three situations, i.e., one-dimensional unidirectional flow, egress process and queuing process. Experimental, theoretical and simulation results, which give us some prescriptions of easing jam in the situations above, are presented.

### 20.1 Introduction

“Jamology” is an interdisciplinary study on self-driven particles such as vehicles, pedestrians, ants, molecular motors, and many others [1]. It has characteristics of both physics and engineering. Its goal is not only elucidation of collective phenomena of self-driven particles, but also development of solutions for jam, which disrupts smooth flow.

Dynamics of pedestrians, which has been vigorously studied in traffic engineering, architecture and psychology, is also one of the main research topic in Jamology. Pedestrians (self-driven particles) do not obey the law of action and reaction; therefore, Newtonian mechanics does not work effectively. Moreover, it is almost impossible to predict the movement of individual pedestrian in detail since he/she has own will. In spite of these difficulties, researchers have developed new theories and models [1, 2], and studied macroscopic collective behaviors of pedestrians when the destination of pedestrians is clear. Some solutions for ease congestion (jam) are also considered.

In this paper, the author reviews the achievements of research on one-dimensional unidirectional flow, egress (evacuation) process and queuing process. In congested unidirectional flow, slow rhythm improves pedestrian flow [3]. A simple egress model succeeds in explaining the effect of competitive and cooperative behavior at an exit, which has been previously studied by experiment and simulation

---

D. Yanagisawa (✉)

Department of Aeronautics and Astronautics, School of Engineering, The University of Tokyo,  
7-3-1, Hongo, Bunkyo-ku, Tokyo, 113-8656, Japan  
e-mail: [tDaichi@mail.ecc.u-tokyo.ac.jp](mailto:tDaichi@mail.ecc.u-tokyo.ac.jp)

© The Author(s) 2015

H. Takayasu et al. (eds.), *Proceedings of the International Conference on Social Modeling and Simulation, plus Econophysics Colloquium 2014*, Springer  
Proceedings in Complexity, DOI 10.1007/978-3-319-20591-5\_20

219

[4, 5]. In queuing process, the effect of walking distance, which is necessary for modeling pedestrians, are introduced to the original queueing model in the queueing theory[6]. Our extended model succeeds to suggest a suitable type of queueing system as a function of the parameters in queueing systems [7].

## 20.2 Effect of Rhythm on Unidirectional Flow

Unidirectional flow is one of the fundamental situations in pedestrian dynamics; however, it still includes complex phenomena such as overtaking and movement in lateral directions. Therefore, researchers often consider an ideal condition, i.e., one-dimensional circuit where overtaking is prohibited as in Fig. 20.1a. Then they investigate fundamental diagram (FD) as in Fig. 20.1b, which is a relation between flow and density of pedestrians [8, 9]. We mainly see two phases in FD. One is free-flow phase, where flow becomes large against the increase of density. The other is congested phase, where flow becomes small against the increase of density.

In [10] the effect of music on an individual pedestrian has been studied experimentally. Inspired by this research, we analyze the effect of rhythm on crowded pedestrians experimentally and reveal that *slow* rhythm increases pedestrian flow in congested situations without any danger.

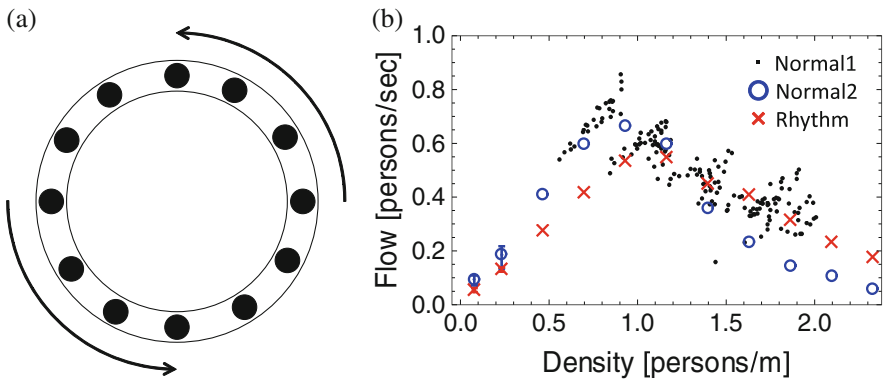


**Fig. 20.1** (a) Schematic view of one-dimensional unidirectional pedestrian flow in a circuit. (b) Fundamental diagram. Normal1 is data in [8]. Normal2 and Rhythm are data in [3]

### 20.2.1 *Experimental Setup*

We constructed a circuit whose inner and outer radii were  $r_i = 1.8$  [m] and  $r_o = 2.3$  [m], respectively. The participants of the experiment, who were male university students between 18 and 39 years old, walked the circuit in the counter-clockwise direction. In the beginning of each trial, we briefly instructed participants to distribute homogeneously in the circuit without signs on the floor or measuring the distance between each participant.

We executed 11 kinds of density conditions. The number of the participants in the circuit in each condition was  $N = \{1, 3, 6, 9, \dots, 30\}$ . The conditions  $N = 1$  and  $N = 3$  were tried three times with different participants, and the other conditions were tried once. Each trial was more than 1 min in the cases  $N \geq 3$ . The global density is calculated as

$$\frac{N}{\pi (r_i + r_o)} \quad (20.1)$$

and was used to depict FDs.

Two kinds of walking were performed in the experiment. In the first case, we did not give any specific instructions to the participants, so that they walked normally. In the latter case, the participants were instructed to walk with the sound from the electric metronome, whose rhythm is 70 [BPM]. Note that we did not inform which foot to move first.

In the case  $N = 1$ , we measured the lap time for completing a circuit. In the case  $N \geq 3$ , we measured the time that each participant passes the measuring point in the circuit and depicted the cumulative plots, which show the evolution of the total number of participants who passed the measuring point. Then, linear regression analysis gives pedestrian flows as the slope of the cumulative plots. The condition  $N = 1$  and 3 (the smallest and the second smallest density case) were performed three times so that the maximum and minimum values are plotted by the error bars in Fig. 20.1. In the case  $N \geq 6$ , the errors obtained from the linear regression analysis is too small to be depicted by error bars.

### 20.2.2 *Experimental Verification of the Effect of Rhythm*

Figure 20.1b shows the FDs obtained in our experiment (Normal2 and Rhythm). From the figure, first, we see that the flow is larger in the normal case than the rhythmic case in the low-density regime. Hence, the pace 70 [BPM] is much slower than the normal-walking pace of the participants, and the flow becomes smaller if the participants try to walk with the slow rhythm. Second, linearity of the flows in the low-density regime verified that participants walked with constant step size and pace. Third, we see that the flow decreases linearly in the rhythmic case,

whereas, the flow in the normal case is convex downward in the high-density regime. This observation is supported by calculating average second difference of the data between  $N = 15$  and  $30$ , which are  $0.14$  and  $0.03$  in the normal and rhythmic cases, respectively. We consider that the clear convexity, which was not seen in the FD in [8] (Fig. 20.1b Normal1), is observed because we performed the experiment with a density of more than  $2.0$  [persons/m]. In [3], these experimental data are compared with (fitted by) the mathematical model. They indicates that linear decreasing of the flow implies that step size of pedestrians becomes smaller. On the other hand, convexity indicates that both step size and pace become smaller. Thus, the walking pace decreases from the influence of the predecessors in the normal case, while it is maintained by rhythm in the rhythmic case. Finally, we observe the crossing of the two plots. In other words, the flow of the rhythmic case exceeds that of the normal case in the high-density regime. Therefore, we have verified that slow rhythm improves the pedestrian flow.

### 20.3 Simple Model of Egress Process

Egress process is vigorously studied since it is strongly related with evacuation in emergency situation. Many simulations as well as experiments by real pedestrians are performed [5, 11]; however, there are few theoretical research [12]. In this section, we introduce a simple model, which explains the effect of competitive and cooperative behavior near an exit.

We consider a system, which is composed of an exit cell and its Moore neighboring cells as in Fig. 20.2a. Time is discrete in this model. It is assumed that pedestrians come from the outside of the system, and at each five neighboring cell, there is a pedestrian with the probability  $\sigma$ . They try to move to the exit cell with the

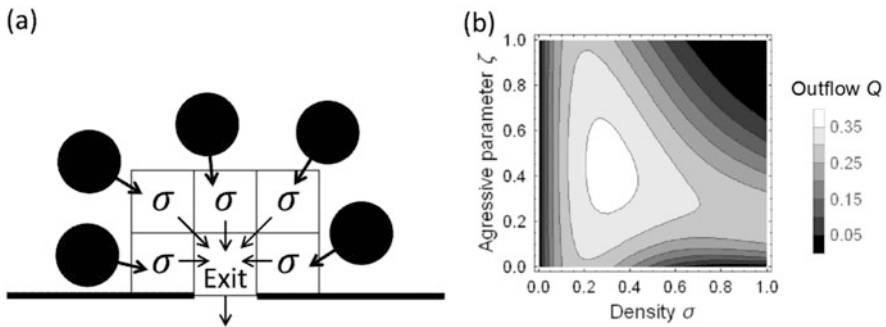


Fig. 20.2 (a) Schematic view of a simple egress model. (b) Contour plot of outflow  $Q$

probability 1 if it is not occupied by others.<sup>1</sup> The pedestrian at the exit cell get out from the system with the probability 1. We denote the number of the neighboring cells by  $n$ . (Here  $n = 5$ .) Then the probability of  $m$  pedestrians trying to move to the exit cell is described by the binomial distribution as follows.

$$b(m) = \binom{n}{m} \sigma^m (1 - \sigma)^{n-m} \quad (20.2)$$

If more than one pedestrian try to move to the exit cell, conflict occur since only one pedestrian can stay at the exit cell. Thus, we introduce frictional function, which is the probability that no one can move to the exit cell.

$$\psi(m) = \begin{cases} 0 & (m = 0, 1) \\ 1 - m\zeta(1 - \zeta)^{m-1} & (m \geq 2) \end{cases}, \quad (20.3)$$

where  $\zeta$  is the aggressive parameter, which is the probability that the pedestrians trying to move to the exit cell in spite of the conflict among them. The parameter  $\zeta$  represents the competitiveness of the pedestrians. If  $\zeta$  is small, pedestrians are in cooperative mood and often give way to each other. By contrast, pedestrians are in competitive mood and collide with each other at the exit when  $\zeta$  is large. The second term in the second line in Eq. (20.3) corresponds to the situation that one pedestrian aggressively move to the exit cell and the other  $m - 1$  pedestrians give way to others. By subtracting this term from 1, we calculate the probability that no one can move. Furthermore, Eq. (20.3) indicates that if all the pedestrians give way to others, no one moves to the exit cell. By using Eqs. (20.2) and (20.3), the probability that one pedestrian reaches the exit cell is calculated as

$$r(n) = \sum_{m=1}^n (1 - \psi(m)) b(m). \quad (20.4)$$

We denote the probabilities that the exit cell is vacant and occupied by  $P(0)$  and  $P(1)$ , respectively. Then, the master equations in the stationary state are described as

$$\begin{bmatrix} P(0) \\ P(1) \end{bmatrix} = \begin{bmatrix} 1 - r(n) & 1 \\ r(n) & 0 \end{bmatrix} \begin{bmatrix} P(0) \\ P(1) \end{bmatrix} \quad (20.5)$$

We solve Eq. (20.5) with the normalization condition  $P(0) + P(1) = 1$  and obtain the expression of pedestrian outflow.

$$Q(\sigma, \zeta, n) = 1 \cdot P(1) = \frac{r(n)}{1 + r(n)}. \quad (20.6)$$

---

<sup>1</sup>If we introduce the moving probability from the neighboring cells to the exit cell, which is 1 in this paper, we can represent slow and first pedestrians.

Figure 20.2b is contour plot of the outflow  $Q$  in the case  $n = 5$ . When  $\sigma < 0.2$ , few conflicts occur, so that the outflow  $Q$  is hardly affected by the aggressive parameter  $\zeta$ . When  $\sigma > 0.2$ , conflicts occur more often, so that  $Q$  achieves maximum against the change of  $\zeta$  with constant  $\sigma$ . Few pedestrians move to the exit cell in a conflict situation in the small  $\zeta$  case since they often give way to others. On the contrary, a conflict among aggressive pedestrians is not solved in the large  $\zeta$  case. Therefore, both small and large  $\zeta$  diminish the outflow  $Q$ . It is interesting that the simple model introduced in this section succeed to show the existence of the optimal strength of giving way to others.

In [4], the effect of competitive and cooperative behavior on evacuation is experimentally studied. It indicates that pedestrians can evacuation faster when they are in cooperative mood if the width of the exit is narrow. This result corresponds to our result in Fig. 20.2. In the experimental evacuation process, it is feasible to consider that the density around the exit is large, i.e.,  $\sigma$  is large. Figure 20.2b implies that the outflow achieves maximum at small  $\zeta$ , i.e., cooperative mood, when density is large.

## 20.4 Queuing Process

Pedestrian queueing system, which we see at cash registers in super markets, ticket-vending machines in stations, and automated teller machines in banks, is also one of the important themes in the field of pedestrian dynamics for the following reasons. Firstly, pedestrians become stressful when they wait at a queue for a long time. Secondly, long waiting time in one queueing system affects the starting time of other events, for instance, if some passengers take a long time to pass a security check in an airport due to a long waiting queue, the departure time of the flight may delay [13]. Lastly, a long queue prevents smooth movement of pedestrians and encourages forming a jam around it. Thus, we investigate efficient type of pedestrian queueing system in this section.

According to the queueing theory [6], mean waiting time (MWT) in the fork-type queueing system (Fork) is always shorter than that in the parallel-type queueing system (Parallel). However, in the queueing theory, the effect of walking distance from the head of the queue to the service windows is not included. The effect of the distance may significantly influences on the MWT of pedestrians in large Fork such as an immigration inspection floor in an international airport where walking distance is very long. Therefore, we have developed a walking-distance introduced Parallel (D-Parallel, Fig. 20.3a) and a walking-distance introduced Fork (D-Fork, Fig. 20.3b). We show that MWT becomes shorter in D-Parallel than D-Fork when sufficiently many pedestrians are waiting in the queue.

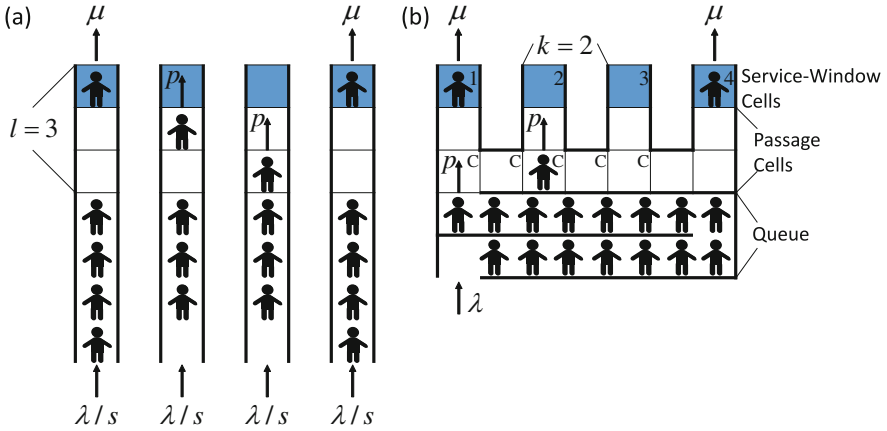


**Fig. 20.3** Schematic view of walking-distance introduced queueing model. (a) D-Parallel. (b) D-Fork

### 20.4.1 Walking-Distance Introduced Parallel-Type Queueing System: D-Parallel

D-Parallel (Fig. 20.3a) is divided into three parts, which are queues, passage cells, and service-window cells (SWCs). The number of SWCs are denoted by  $s$ . The SWCs have two states: vacant and occupied. Note that each cell contains only one pedestrian at most. Time is discrete in the model. A pedestrian arrives at the queueing system (each queue) with the probability  $\lambda$  ( $\lambda/s$ ). When a SWC becomes vacant state, a pedestrian at the head of the queue decides to proceed to the SWC, and it becomes occupied state. The pedestrian walks passage cells to the SWC for  $l$  cells with probability  $p$  and starts receiving the service.<sup>2</sup> It finishes with the probability  $\mu$  and the pedestrian leaves the system. At the same time the SWC becomes vacant state again. The walking effect delays the start of service and affects MWT. Note that the size of the SWCs is considered as one cell in our model, so that  $l \geq 1$  is satisfied in D-Parallel. Besides, we focus on the situation that  $p > \lambda$ ,  $\mu$ , which is natural for queueing situation.

<sup>2</sup>The parameter  $p$  controls the walking velocity of pedestrians. If we set  $p$  to small value, we can consider slow pedestrians, who are greatly affected by long walking distance. In this paper, it is fixed to  $p = 1$  in the simulation, so that fast pedestrians are considered.

### 20.4.2 *Walking-Distance Introduced Fork-Type Queueing System: D-Fork*

D-Fork is divided into three parts as D-Parallel. Firstly, the place where pedestrians are waiting, which is not divided into cells, is a queue. Secondly, the cells in the middle part are passage cells. The passages cells with the letter “C” in Fig. 20.3b are common passage cells, where multiple pedestrians pass during the transfer to the SWCs. In contrast, the passage cells with no letter are normal passage cells, which lead to only one SWC. Finally, the cells with the numbers are SWCs.

The parameters  $\lambda$ ,  $\mu$ ,  $p$  ( $\in (0, 1]$ ), and  $s$  ( $\in \mathbb{N}$ ) represent the arrival probability, the service probability, the walking probability, and the number of service windows, respectively, as similar to D-Parallel. The longitudinal distance from the head of the queue to the service windows are given by  $l$ . Besides, the interval distance between two service windows is given by  $k$ . Figure 20.3b represents the case where  $s = 4$ ,  $l = 3$ , and  $k = 2$ .

Outline of the movement of pedestrians and the state transition of the SWCs are as follows (Details are described in Sect. 20.4.3). A pedestrian arrives at the queueing system with the probability  $\lambda$ . When he/she reaches the head of the queue and there is at least one vacant SWC, he/she decides to move to it, and its state changes into occupied state. The pedestrian proceed to the SWC by one cell with the probability  $p$  in one time step if his/her proceeding cell is vacant. A service starts when the pedestrian arrives at the SWC, and after it finishes with the probability  $\mu$  the state of the SWC changes into the vacant state.

### 20.4.3 *Update Rule in Simulation*

The simulation of D-Parallel and D-Fork consists of the following five steps per unit time step.

1. If the following three conditions:

- there is at least one pedestrian in the queue,
- target SWC of the pedestrian at the head of the queue is not determined,
- there is at least one SWC in the vacant state,

are satisfied, the pedestrian at the head of the queue decides to proceed to the nearest vacant SWC, and the state of the SWC becomes occupied. Note that he/she never changes the target SWC even if some other SWCs which are nearer than his/her target become vacant state during his/her walking process.

2. Add one pedestrian to the queue with the probability  $\lambda$ .

3. If the target SWC of the pedestrian at the head of the queue is determined and the first cell of the passage cell is vacant, proceed him/her to the first passage cell with the probability  $p$ .

4. Proceed each pedestrian in the passage cells (except the pedestrian who moved in the step 3) by one cell to his/her service windows with the probability  $p$  if there is no pedestrian at their proceeding cell.
5. Remove pedestrians at the SWCs (except the pedestrian who reach the SWC in the step 4) and change their states into vacant state with the probability  $\mu$ .

### 20.5 Comparison of Mean Waiting Time in D-Parallel and D-Fork

Figure 20.4 show MWT against arrival-service ratio  $\rho (= \lambda/(s\mu))$ . We clearly observe the crossing of the curves of D-Parallel and D-Fork. This indicates that when the arrival-service ratio  $\rho$  is small, i.e., there are not frequent arrival of pedestrians against total service efficiency of the system; we should form D-Fork to decrease MWT. On the contrary, when  $\rho$  is large, i.e., pedestrians arrive frequently against total service efficiency of the system, we should form D-Parallel.

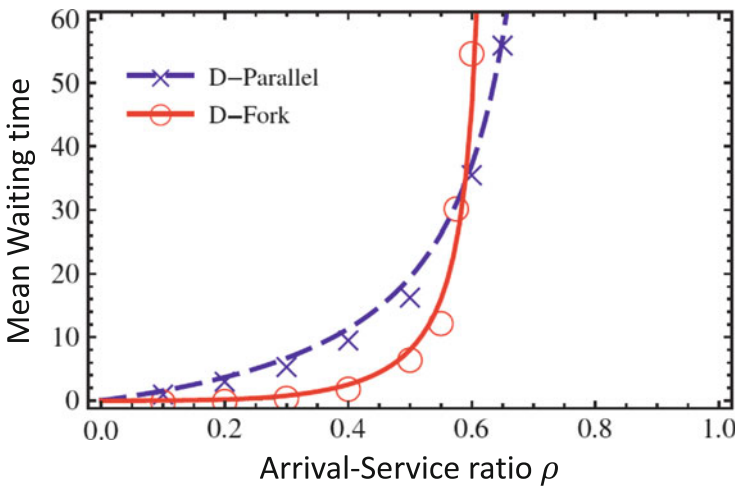


**Fig. 20.4** Mean waiting time against arrival-service ratio  $\rho$  in the case  $\mu = 0.1$  and  $p = 1$ . The marker plots are the result of our simulation and the solid and dashed lines are result of approximated theoretical analysis in [7]

## 20.6 Summary

In this paper, we briefly review our result in pedestrian dynamics. We have discovered that slow rhythm improves pedestrian flow in congested situation. Our simple theoretical model well explains the effect of competitive and cooperative behavior at a narrow exit on outflow. Simulation of walking-distance introduced queueing models indicates that the fork-type is not always the suitable type for pedestrian queueing system.

Egress process is studied in more detail. A simple egress model introduced in Sect. 20.3 also helps explaining the effect of an obstacle at a narrow exit [11]. It is also revealed that diminution of local flow enhance the total flow at the exit in the case there are successive bottlenecks [14].

In the near future, combined topics such as the effect of rhythm on the egress process should be also studied. Furthermore, as we have investigated suitable type of queueing system, effective room arrangement and position of exits for egress process is needed to be considered. It is expected that application of our results will diminish “jams” in the real world.

**Acknowledgements** This work was supported by JSPS KAKENHI Grant Number 24760058.

**Open Access** This book is distributed under the terms of the Creative Commons Attribution Non-commercial License which permits any noncommercial use, distribution, and reproduction in any medium, provided the original author(s) and source are credited.

## References

- Schadschneider A, Chowdhury D, Nishinari K (2010) Stochastic transport in complex systems. Elsevier, Amsterdam/Oxford
- Helbing D (2001) Rev Mod Phys 73(4):1067 doi:[10.1103/RevModPhys.73.1067](https://doi.org/10.1103/RevModPhys.73.1067)
- Yanagisawa D, Tomoeda A, Nishinari K (2012) Phys Rev E 85(1):016111. doi:[10.1103/PhysRevE.85.016111](https://doi.org/10.1103/PhysRevE.85.016111)
- Muir HC, Bottomley DM, Marrison C (1996) Int J Aviat Psychol 6(1):57 doi:[10.1207/s15327108ijap0601\\_4](https://doi.org/10.1207/s15327108ijap0601_4)
- Kirchner A, Klüpfel H, Nishinari K, Schadschneider A, Schreckenberg M (2003) Phys A Stat Mech Appl 324(3–4):689 doi:[10.1016/S0378-4371\(03\)00076-1](https://doi.org/10.1016/S0378-4371(03)00076-1)
- Bolch G, Greiner S, de Meer H, Trivedi KS (2006) Queueing networks and Markov chains: modeling and performance evaluation with computer science applications, 2nd edn. Wiley, Hoboken.
- Yanagisawa D, Suma Y, Tomoeda A, Miura A, Ohtsuka K, Nishinari K (2013) Transp Res C Emerg Technol 37:238 doi:[10.1016/j.trc.2013.04.008](https://doi.org/10.1016/j.trc.2013.04.008)
- Seyfried A, Steffen B, Klingsch W, Boltes M (2005) J Stat Mech Theory Exp 2005(10):P10002. doi:[10.1088/1742-5468/2005/10/P10002](https://doi.org/10.1088/1742-5468/2005/10/P10002)
- Jelić A, Appert-Rolland C, Lemerrier S, Pettré J (2012) Phys Rev E 85(3):036111. doi:[10.1103/PhysRevE.85.036111](https://doi.org/10.1103/PhysRevE.85.036111)
- Styns F, van Noorden L, Moelants D, Leman M (2007) Hum Mov Sci 26:769 doi:[10.1016/j.humov.2007.07.007](https://doi.org/10.1016/j.humov.2007.07.007)

11. Yanagisawa D, Kimura A, Tomoeda A, Nishi R, Suma Y, Ohtsuka K, Nishinari K (2009) Phys Rev E 80(3):036110. doi:[10.1103/PhysRevE.80.036110](https://doi.org/10.1103/PhysRevE.80.036110).
12. Yanagisawa D, Nishinari K (2007) Phys Rev E 76(6):061117. doi:[10.1103/PhysRevE.76.061117](https://doi.org/10.1103/PhysRevE.76.061117).
13. Kazda A, Caves RE (2007) Airport design and operation, 2nd edn. Elsevier, Oxford
14. Ezaki T, Yanagisawa D, Nishinari K (2012) Phys Rev E 86(2):026118. doi:[10.1103/PhysRevE.86.026118](https://doi.org/10.1103/PhysRevE.86.026118).